Laboratori Nazionali di Frascati

LNF-65/49

R. Gatto :

THEORETICAL ASPECTS OF COLLIDING BEAM EXPERIMENTS

Estratto da: Springer Tracts in Modern Physics (Springer, Berlin, 1965) vol. 39, pag. 106.

Theoretical Aspects of Colliding Beam Experiments

R. Gatto

Istituto di Fisica
dell'Università, Firenze
Laboratori Nazionali del
C. N. E. N. di Frascati, Roma

In this talk I shall try to summarize the theoretical aspects of colliding beam experiments. I shall try to be rather elementary, as this talk should be intended mostly for those who will do experiments with colliding beams.

The following table shows a list of colliding beam projects at different laboratories which are either completed or in construction or still under study.

Table 1

$e^+ e^-$				
Frascati	AdA	$e^+ e^-$	250 MeV	working
Moscow	FIAN	$e^+ e^-$	270 MeV	
Orsay	ACO	$e^+ e^-$	450 MeV	to be completed
Novosibirsk		$e^+ e^-$	700 MeV	to be completed
Frascati	Adone	$e^+ e^-$	1500 MeV	in construction
Stanford		$e^+ e^-$	3000 MeV	project
Cambridge		$e^+ e^-$	3000 MeV	study
Erevan		$e^+ e^-$	3000 MeV	study
Hamburg		$e^+ e^-$		study
$e^- e^-$				
Kharkov		$e^- e^-$	100 MeV	to be completed
Novosibirsk		$e^- e^-$	130 MeV	working
Stanford		$e^- e^-$	500 MeV	working

The topics I shall discuss are:

Electromagnetic reactions: $e^+ + e^- \to 2\gamma$, $e^+ + e^- \to e^+ + e^-$, $e^+ + e^- \to e^+ + e^- + \gamma$, $e^+ + e^- \to \mu^+ + \mu^-$, $e^- + e^- \to e^- + e^-$, $e^- + e^- \to e^- + e^- + \gamma$, etc.; vacuum polarization effects; $e^- - e^+$ annihilation

into strong interacting particles; the one-photon channel; resonant contributions; annihilation into pions; intermediate ρ^0, ω^0, and φ^0; two-photon channel; annihilation into fermion-pairs; weak-vector-meson production and weak interactions.

1. Colliding $e^- - e^-$ and $e^+ - e^-$ beams can be used to test electrodynamics. Unfortunately for an evaluation of the tests one would need a model for the breakdown. The usual procedure of modifying the propagators [1] has a great disadvantage in its lack of gauge-invariance.

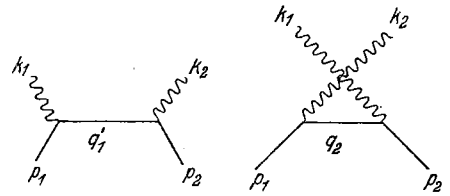

Fig. 1. Graphs for $e^+ + e^- \to 2\gamma$

A recent paper by DRELL and MCCLURE [2] discusses a better model of breaking but contains more form factors. In view of these facts our considerations on tests of quantum electrodynamics will be openly superficial and only of indicative value.

I shall first discuss the electromagnetic reactions

$$e^+ + e^- \to 2\gamma \tag{1}$$

$$e^+ + e^- \to e^+ + e^- \tag{2}$$

$$e^+ + e^- \to e^+ + e^- + \gamma \tag{3}$$

$$e^+ + e^- \to \mu^+ + \mu^- . \tag{4}$$

2. Reaction (1) occurs in lowest order through the graphs (Fig. 1) In c. m.

$$q_1^2 = 4E^2 \sin^2 \frac{\theta}{2}$$

$$q_2^2 = 4E^2 \cos^2 \frac{\theta}{2}$$

where E is the c. m. energy of e^- (or e^+) and θ is the annihilation angle. In the relativistic limit and for $\theta \gg (m_e/E)$

$$\frac{d\sigma}{d(\cos\theta)} = (\pi r_0^2) \left(\frac{m_e}{E}\right)^2 \frac{|F(q_1^2)|^2 \cos^4 \frac{\theta}{2} + |F(q_2^2)|^2 \sin^4 \frac{\theta}{2}}{\sin^2\theta} \tag{5}$$

where r_0 is the electron radius and we have introduced a form factor $F(q^2)$, depending on the transferred momentum, to account for possible breaking of the theory. The form factor F can be thought as a product, $F = V_e^2 P_e$, of a form factor for the electron vertex and a form factor for the electron propagator. If $F = 1$ from (5) one gets

$$\frac{d\sigma}{d(\cos\theta)} = (\pi r_0^2) \left(\frac{m_e}{E}\right)^2 \frac{1}{2} \frac{2 - \sin^2\theta}{\sin^2\theta} \tag{6}$$

which holds, like (5) for $\theta \gg (m_e/E)$. For θ near 0°

$$\frac{d\sigma}{d(\cos\theta)} = (\pi r_0^2)\left(\frac{m_e}{E}\right)^2 \frac{1}{\sin^2\theta + \left(\frac{m_e}{E}\right)^2 \cos^2\theta} . \tag{7}$$

We have plotted in Fig. 2 the differential cross-section for various energies E. The total cross-section is given by

$$\sigma = (\pi r_0^2)\left(\frac{m_e}{E}\right)^2 \left(\log\frac{2E}{m_e} - \frac{1}{2}\right) . \tag{8}$$

Let us take

$$F(q^2) = \frac{1}{1 + \frac{q^2}{Q^2}} . \tag{9}$$

One finds for $Q = 1$ GeV (corresponding to 0.2 fermi) that the cross-section at $E = 250$ MeV is changed from its value with $F = 1$ as follows:

at 90° by −12%
60° − 7%
45° − 4%
30° −0.7% .

Thus, very roughly, at $E = 250$ MeV, if one can distinguish a 7% effect at 60° one can test the theory to 0.2 fermi. If $E = 500$ MeV a similar

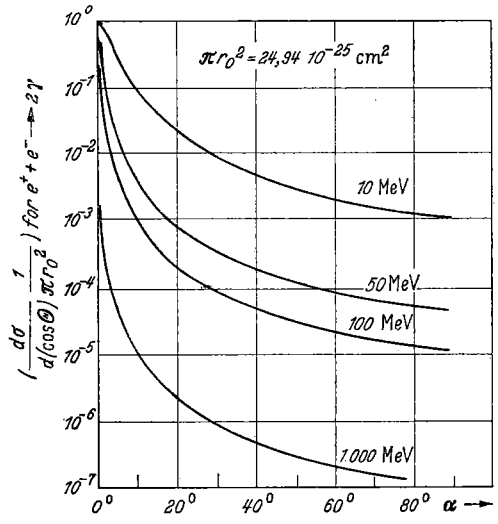

Fig. 2. Differential cross-section of $e^+ + e^- \to 2\gamma$ in lowest order

experiment would test the theory to 0.1 fermi, according to this model where the effect depends on $(E/Q)^2$. Similarly if $E = 1$ BeV the test is up to 0.05 fermi. The use of reaction (1) as a monitoring process for beam collisions is unfortunately not convenient. The monitoring process must be such that in the particular geometry it involves only very small

momentum transfers even at the highest energy. It will then be very reliably predicted by the theory, and from the calculated cross-section one can check the beam dimensions by a uniform and instantaneous procedure. The 2γ annihilation at forward angles would be a possible monitor except that its cross-section is too low in that region in comparison to other processes that show a stronger singularity in the forward direction. In particular the process

$$e^+ + e^- \to e^+ + e^- + 2\gamma \tag{10}$$

with the photons going in opposite directions is expected to contaminate the measurement of 2γ annihilation. BAYER and GALITSKY [3] have calculated the cross-section of (10) in a classical approximation. The cross-section of double bremsstrahlung is written as

$$d\sigma_2 = d\sigma_0 \frac{1}{2!} dw(k_1)\, dw(k_2) \tag{11}$$

where

$$dw = \frac{1}{2\omega} j_\mu j^\mu \, d^3k \tag{12}$$

and

$$j_\mu = \frac{i\,e}{(2\pi)^{3/2}} \left[\sum_i \frac{(p_i)_\mu}{(k p_i)} - \sum_j \frac{(p'_j)_\mu}{(k p'_j)} \right] . \tag{13}$$

p_i being the momentum of an incoming particle and p'_j that of an outgoing particle [4]. For the case considered, BAYER and GALITSKY give the result (in c. m.)

$$\frac{d\sigma(e^+ + e^- \to e^+ + e^- + 2\gamma)}{d\sigma(e^+ + e^- \to 2\gamma)} = \frac{2.3 \times 32\, \alpha^2 \gamma^2}{\pi^2 \ln 2\gamma} \frac{d\omega_1}{\omega_1} \frac{d\omega_2}{\omega_2} \tag{14}$$

where $\gamma = E/m_e$, and ω_1 and ω_2 are the photon energies. Eq. (14) shows that 2γ bremsstrahlung will be larger than 2γ annihilation at sufficiently high energy, in the approximation used. A complete calculation of 2γ bremsstrahlung, including a complete calculation of hard photon emission, has not however been made so far. The radiative corrections of $e^+ + e^- \to 2\gamma$ have been recently calculated by TSAI [5]. TSAI is interested in the possible use of $e^+ + e^- \to 2\gamma$ to produce high energy γ-rays. He therefore calculates the spreading of the photon peak at a fixed angle in positron-hydrogen-atom collisions, which arises from radiative corrections. The radiative corrections obtained by TSAI do not contain dangerous terms of the kind $(\alpha/\pi) \ln^2(4E^2/m_e^2)$ which cancel out after addition of the elastic and the inelastic contributions. Such $\ln^2$-terms had been found in previous calculations but their appearance was due to the unnatural choice of phase-space for the additional bremsstrahlung photon which had been supposed to include energies ω_3 up to a maximum value $\ll m_e$ and isotropic in the laboratory system. Terms of the kind $(\alpha/\pi) \ln^2(4E^2/m_e^2)$ would become of the order of unity at energies of the order of a few BeV thus making the whole perturbative approach unvalid, for instance when interpreting a high energy $e^+ - e^-$ colliding beam experiment. The phase-space for the bremsstrahlung photon is

dictated by the experimental set-up of the particular experiment. TSAI gives for the radiative correction δ, defined by

$$\frac{\mathrm{d}\sigma}{\mathrm{d}\Omega} = \frac{\mathrm{d}\sigma_0}{\mathrm{d}\Omega}(1+\delta) \tag{15}$$

the expression

$$\delta = -\frac{2\alpha}{\pi}\left\{\left(\ln\frac{E}{K_3^{\max}} - \frac{3}{4}\right)\left(\ln\frac{4E^2}{m_e^2} - 1\right) + \frac{f}{2}\right\} \tag{16}$$

where f is a complicated function, usually rather small in the experimental conditions. The cut-off $K_3^{\max}$ is to be calculated from the energy and angular resolution of the detectors. Eq. (16) has a striking similarity to Schwinger's radiative corrections to potential scattering.

$$\delta_{\text{Schwinger}} \approx -\frac{2\alpha}{\pi}\left\{\left(\ln\frac{\mathscr{E}}{\Delta\mathscr{E}} - \frac{13}{12}\right)\left(\ln\left(\frac{-q^2}{m_e^2}\right) - 1\right) + \frac{17}{36}\right\} \tag{17}$$

provided one substitutes

$$\frac{\mathscr{E}}{\Delta\mathscr{E}} \to \frac{E}{K_3^{\max}} \quad \text{and} \quad -q^2 \to 4E^2 .$$

TSAI notices that the two expressions become almost identical if one subtracts the vacuum polarization contribution from Schwinger's δ, corresponding to the fact that there are no such contributions in the annihilation problem. A calculation of the radiative corrections to the total $e^+ + e^- \to 2\gamma$ cross-section has also been performed by ANDREASSI et al. [6]. Actually ANDREASSI et al. calculate the total cross-section for $e^+ - e^-$ annihilation into photons to order e^6 (i. e. annihilation into 2γ and 3γ)

$$\sigma_{\text{tot}} = \sigma_D(1 + \delta_T)$$

where σ_D is the Dirac $e^+ + e^- \to 2\gamma$ cross-section. In the E. R. limit they find

$$\delta_T = \frac{\alpha}{12\pi}\left[2\ln^2 2\gamma - \ln 2\gamma + (4\pi^2 - 13) - \frac{5\pi^2 - 11}{\ln 2\gamma - 1}\right] .$$

The presence of the $\ln^2(2\gamma)$ term is the most significant result. A theorem by ERIKSSON and PETERMAN [7] says that the radiative corrections to a differential cross-section for large values of the squared momentum transfer in c. m. (calculated from soft photons) are expandible in a power series of $(\alpha/\pi)\ln(q^2/m^2)$. Specifically for $q^2 \gg m^2$ in c. m., to order e^6, according to this theorem one expects

$$\delta = \frac{\alpha}{\pi}\left[c_1 \ln\frac{E}{\Delta E}\ln\frac{q^2}{m^2} + c_2 \ln\frac{q^2}{m^2} + c_3\right]$$

where c_1, c_2, c_3 are angle-dependent. Addition of hard photons may add terms $\ln^2(E/\Delta E)$ but not modify the main conclusion. According to ANDREASSI, BUDINI and FURLAN the $\ln^2(2\gamma)$ comes from the region of small q^2 (where the theorem does not hold) and precisely from soft photons.

3. The reaction (2), electron-positron scattering, is obtained in lowest order from the graphs of Fig. 3. In c. m.

$$q_1^2 = 4E^2 \sin^2 \frac{\theta}{2}$$
$$K^2 = -4E^2$$

(q_1 is spacelike, K is timelike). For angles $\theta \neq 0$ and in the relativistic limit

$$\frac{d\sigma}{d(\cos\theta)} = (\pi r_0)^2 \left(\frac{m_e}{E}\right)^2 \left\{ \frac{1}{4} \frac{1 + \cos^4 \frac{\theta}{2}}{\sin^4 \frac{\theta}{2}} |F(q_1^2)|^2 - \frac{1}{2} \frac{\cos^4 \frac{\theta}{2}}{\sin^2 \frac{\theta}{2}} \times \right.$$
$$\left. \times \operatorname{Re}[F(q_1^2) F^*(K^2)] + \frac{1}{8}(1 + \cos^2\theta) |F(K^2)|^2 \right\} \tag{18}$$

We have introduced a form factor F which can be thought of as a product $V_e^2 P_\gamma$ of the electron vertex squared and of the photon propagator.

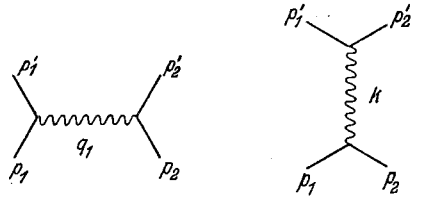

Fig. 3. Graphs for $e^+ + e^- \to e^+ + e^-$

This time V_e refers to a situation where the electron lines are on the mass-shell and the photon is off-mass-shell. On the other hand in the 2γ annihilation of Fig. 1 the incident electron and the photon were on mass-shell and the final electron was off-mass-shell. The two form-factors could then strictly be different. Graphs for $F = 1$ are reported in Fig. 4. At small angle the cross-section arises from transfer of very small momentum. In fact the annihilation graph in Fig. 3 is not singular in the forward direction. The scattering graph dominates in that region and the transferred momentum $q_1^2 \to 0$. Unfortunately, the use of $e^+ - e^-$ scattering as a monitoring process is made difficult just by the singularity of the cross-section at $\theta = 0°$. The dependence on the geometry of the apparatus would be too critical because of the rapid variation of the cross-section. At larger angles, $e^+ - e^-$ scattering can be measured and used for testing the theory. We have reported in Fig. 5 the relative correction to the differential $e^+ - e^-$ cross-section calculated from Eq.(18) with

$$F(q^2) = \frac{1}{1 + \frac{q^2}{Q^2}}$$

for $Q^{-1} = 0.1$ fermi and $Q^{-1} = 0.3$ fermi and for various energy. With a 10% experiment one can measure an effect for $Q^{-1} = 0.3$ fermi

($Q = 670$ MeV) provided one goes at an energy $E \gtrsim 150$ MeV. With the same 10% precision if $Q^{-1} = 0.1$ fermi ($Q = 2$ GeV) one has to go to $E \gtrsim 350$ MeV. With the above choice of $F(q^2)$ the net effect results in a decrease of the cross-section. The maximum deviation would be observed around 90%.

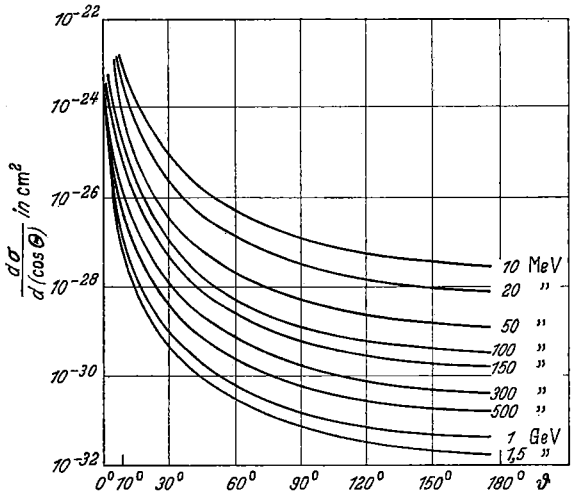

Fig. 4. Differential cross-section for $e^+ + e^- \to e^+ + e^-$ at lowest order

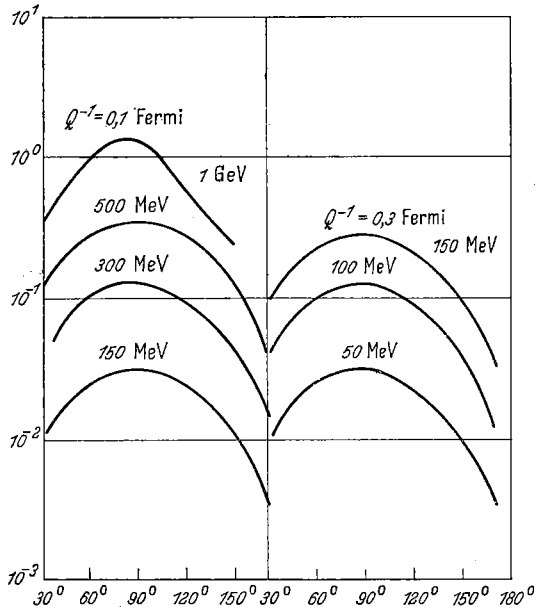

Fig. 5. Relative correction to the differential cross-section for $e^+ + e^- \to e^+ + e^-$ from a simple model of breakdown

4. The reaction (3), $e^+ + e^- \to e^+ + e^- + \gamma$, is the best candidate as a monitoring reaction. As difficulty with such a choice has been considered the fact that the beam can produce γ-rays also by interaction with the residual gas and it would be difficult to separate the two sources on the basis of the shapes of the γ-spectra. However the AdA group [8] has examined the problem and concluded that the separation is indeed possible and poses no relevant problem with machines larger than AdA.

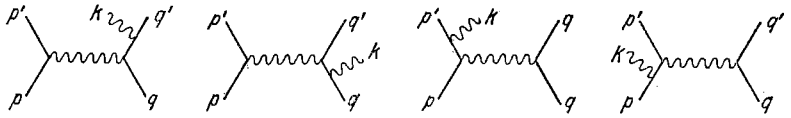

Fig. 6a. Graphs for $e^+ + e^- \to e^+ + e^- + \gamma$: scattering graphs

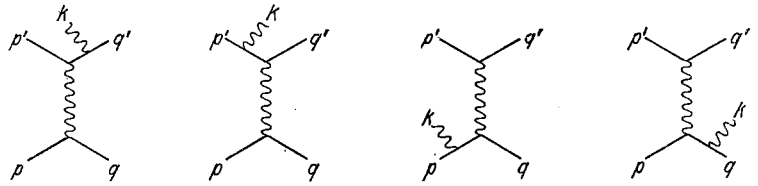

Fig. 6b. Graphs for $e^+ + e^- \to e^+ + e^- + \gamma$: annihilation graphs

The theoretical study of single bremsstrahlung in $e^+ - e^-$ collisions is also of relevance for computing the radiative corrections to $e^+ + e^- \to$ $\to e^+ + e^-$. An evaluation of the radiative corrections of $e^+ + e^- \to$ $\to e^+ + e^-$ implies the integration of the hard photon emission cross-section for those photons which escape detection in the particular experimental situation. There are eight Feynman diagrams for single bremsstrahlung which are reported in Fig. 6a and in Fig. 6b. We call the graphs of Fig. 6a scattering graphs and those of Fig. 6b the annihilation graphs. Single bremsstrahlung calculations have been performed by GARIBYAN [9] and more recently by ALTARELLI and BUCCELLA [10]. These last authors calculate the angular distributions of the photons around the direction of the incident particles after integrating on the final electrons. They also calculate the energy distribution of the emitted radiation and the integrated spectrum from a given c. m. cut-off energy.

Particularly powerful approximations can be made in the region of high energies and small angles of the emitted photon with respect to the colliding beam direction. The annihilation graphs can be neglected in comparison with the scattering graphs on the basis that the denominator of the photon propagator is much smaller for a scattering graph than for an annihilation graph. In a scattering graph the denominator is $(p - p')^2$ or $(q - q')^2$, which for small angle becomes $\sim 4 m_e^6 K_0^2 / W^6$ where W is the total c. m. energy and K_0 is the emitted photon energy. On the other hand in an annihilation graph the denominator is $(p + q)^2 = W^2$ or $(p' + q')^2 = W^2 - 2 W K_0$ and, excluding a small region near the maximum photon energy ($K_{0\max} \sim W/2$), where however the cross-section approaches zero, these denominators are much larger by many orders of magnitudes than those of the scattering graphs. By a different reason one can

neglect the interferences between the first two and the last two graphs of Fig. 6a. In fact the radiation emitted from the electron is contained in a half-cone around the electron line, with an opening angle $\sim m_e/p_0$. The radiation emitted from the positron similarly is in a narrow cone around the positron. There is practically no overlap between the two cones in

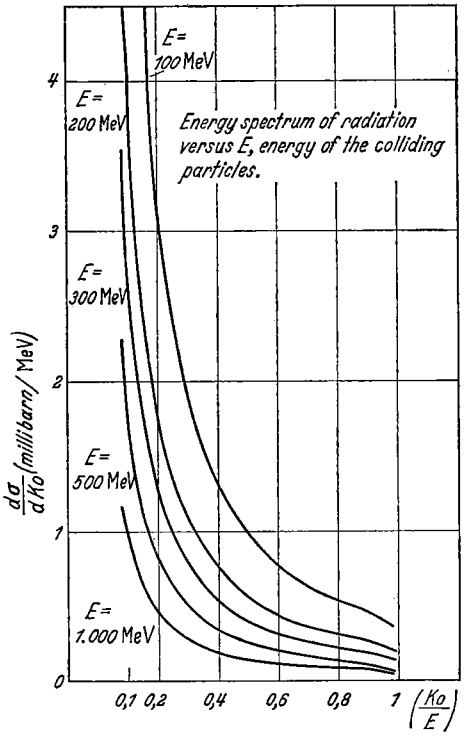

Fig. 7. Bremsstrahlung spectrum for $e^+ + e^- \to e^+ + e^- + \gamma$

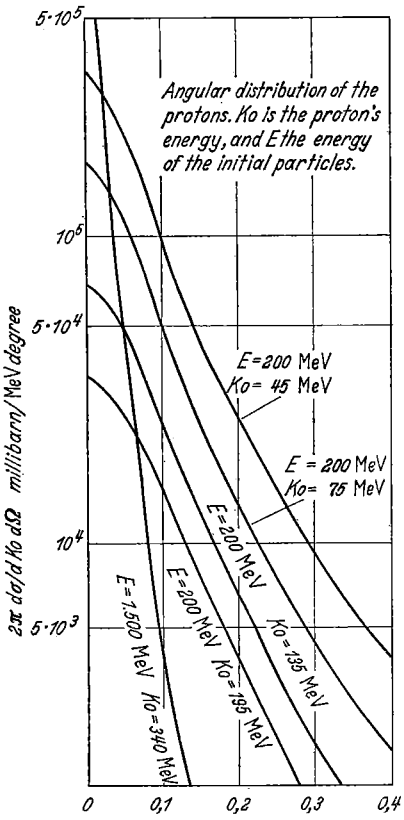

Fig. 8. Angular distribution of bremsstrahlung in $e^+ + e^- \to e^+ + e^- + \gamma$

the most frequent situation of scattering at small angle. Of course, hard photon emission with final electrons at large angles requires a different calculation, as the approximations made here, of neglecting the annihilation graphs, and of neglecting the interference between positron emission and electron emission would have to be improved. In Fig. 8 we report the angular distributions of the photons. The quantity $(2\pi\, \mathrm{d}\sigma)/(\mathrm{d}K_0\, \mathrm{d}\Omega)$ is reported in (millibarn)/(BeV) $\times$ (degree) as a function of the angle between the final photon and the initial positron for $E = 200$ MeV (and various values of K_0) and for $E = 1500$ MeV and $K_0 = 240$ MeV. The energy spectrum $\mathrm{d}\sigma/\mathrm{d}K_0$ can be expressed by

$$\frac{\mathrm{d}\sigma}{\mathrm{d}K_0} \cong 4\alpha r_0^2 \frac{1}{K_0}\left[\frac{2(W^4 + \varrho^4)}{W^4} - \frac{4}{3}\frac{\varrho^2}{W^2}\right]\left[\log\frac{\varrho^2}{2m_e K_0}\frac{W}{m_e} - \frac{1}{2}\right] \quad (19)$$

where r_0 is the electron radius, $W^2 = (p + q)^2$, $\varrho^2 = (p' + q')^2 = W^2 - 2W K_0$ and K_0 is the photon energy. The singularity of the photon spectrum at small K_0 is higher than $1/K_0$ reflecting the singularity of the original process. The integrated spectrum is given by

$$\sigma(\varepsilon) \cong 4\alpha r_0^2 \left\{ \left(\frac{8}{3} \log \frac{W}{2\varepsilon} - \frac{5}{3} \right) \times \right. \\ \left. \times \left(\log \frac{W^2}{m_e^2} - \frac{1}{2} \right) + \frac{4}{3} \left[\log \frac{W}{2\varepsilon} \right]^2 - 1 - \frac{4\pi^2}{q} \right\} . \tag{20}$$

The energy spectrum for $E = 100, 200, 300, 500$ and 1000 MeV is reported in Fig. 7. The spectrum is indeed the typical bremsstrahlung spectrum in the high energy limit in a nuclear field with $Z = 1$ except for an overall factor of two, reflecting the fact that in the $e^+ - e^-$ case two particles can radiate, while in the nuclear case only the electron radiates.

5. Reaction (4), $e^+ + e^- \to \mu^+ + \mu^-$, can be useful also to test muon-structure. At lowest order the reaction proceeds through the graph of Fig. 9. The transferred four-momentum is timelike, $K^2 = -4E^2$. If the electron mass is neglected

$$\frac{d\sigma}{d(\cos\theta)} = \frac{\pi}{4} \alpha^2 \lambda\!\!\!^{-2} \beta_\mu \left[\frac{1}{2} (1 + \cos^2\theta) + \frac{1}{2} \left(\frac{m_\mu}{E} \right)^2 \sin^2\theta \right] F(K^2) \tag{21}$$

where $\alpha = 1/137$, $\lambda\!\!\!^{-}$ is the reduced wavelength of the incoming e^+ (or e^-), β_μ and m_μ are the velocity and mass of the final μ, and we have introduced a form factor F which can be thought of as a product of a muon vertex form-factor V_μ, an electron vertex form-factor V_e, and the photon propagator form-factor P_γ. Note that the angular dependence is not altered by the presence of the form-factor $F(K^2)$. The total cross-section is

$$\sigma = 2.18 \times 10^{-32} \text{ cm}^2 \left[\frac{1}{x^2} \left(1 - \frac{1}{x^2} \right)^{\frac{1}{2}} \left(1 + \frac{1}{2x^2} \right) |F(-4E^2)|^2 \right] \tag{22}$$

with $x = E/m_\mu$. The values of σ for $F = 1$ are reported in Fig. 10 versus x. Fig. 10 also contains the "perturbation theory" cross-sections for $e^+ + e^- \to \pi^+ + \pi^-$, $e^+ + e^- \to p + \bar{p}$, and $e^+ + e^- \to K + \bar{K}$. By "perturbation theory" cross-sections we mean the cross-section one would have for these processes if the strong-interacting particles produced would have no structure (only point-charges). These "perturbation theory" cross-sections are thus quite certainly very far from physical reality, although it may be convenient to know them for purposes of comparison. In Fig. 10 the cross-sections are reported as functions of $x = E/m$, where m is the mass of the particle produced ($m = m_\mu, m_\pi, m_\varrho, m_K$ respectively). To determine a breakdown of the theory in $e^+ + e^- \to \mu^+ + \mu^-$, according to the model of Eq. (21), one has to measure the absolute cross-section. The angular dependence, as we have seen, is independent of a possible breakdown

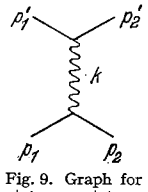

Fig. 9. Graph for $e^+ + e^- \to \mu^+ + \mu^-$

as long as the one-photon channel dominates. For instance with

$$F(q^2) = \frac{1}{1 + \frac{q^2}{Q^2}}$$

the cross-section takes on a factor

$$|F(-4E^2)|^2 \cong 1 + \frac{8E^2}{Q^2}$$

and for $8E^2/Q^2 \sim 10\%$ one can explore up to $Q \sim 9E$, and remembering that 1 GeV corresponds roughly to 0.2 fermi one sees that for $E \sim 300$ MeV

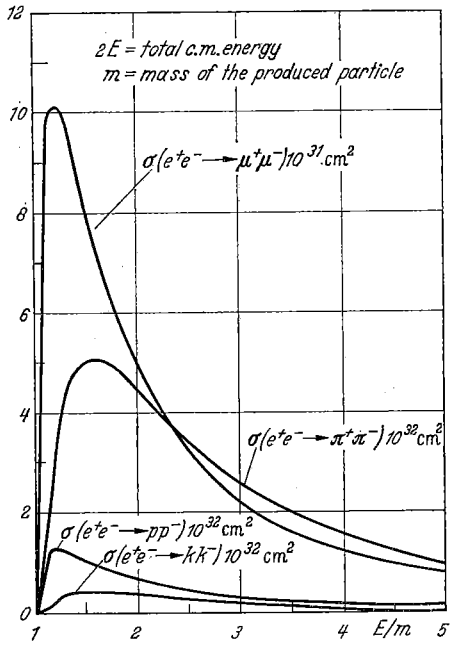

Fig. 10. "Perturbation theory" cross-sections

one can explore already up to $Q \gtrsim 0.1$ fermi and for $E \sim 1$ GeV one can explore up to $Q \gtrsim 0.03$ fermi. In view of its simpler feasibility, annihilation into a muon pair, $e^+ e^- \to \mu^+ \mu^-$, looks as one of the most promising experiments with electron-positron colliding beams. The interpretation of the experiments will require an accurate evaluation of the radiative corrections. These have been discussed by FURLAN, GATTO and LONGHI [11]. Hard photon emission $e^+ + e^- \to \mu^+ + \mu^- + \gamma$ has been discussed by MOSCO [12] and by LONGHI [13]. The graphs contributing to lowest order radiative corrections to $e^+ + e^- \to \mu^+ + \mu^-$ are reported in Fig. 11. Initial and final vertex graphs are denoted by (V_i) and (V_f) respectively. Self-energy graphs are denoted by (SE_i) and (SE_f). Bremsstrahlung graphs are denoted by (B_i) and (B_f). The

two-photon-exchange graphs are called (2γ). One has to add coherently the V, SE, and 2γ graphs to the lowest order graph and then add incoherently the bremsstrahlung contributions. A great simplification occurs if one is interested in experiments that treat symmetrically the final charges (total cross-section, or any arrangement which does not distinguish between μ^+ and μ^-, etc.). In this case (experimentally the

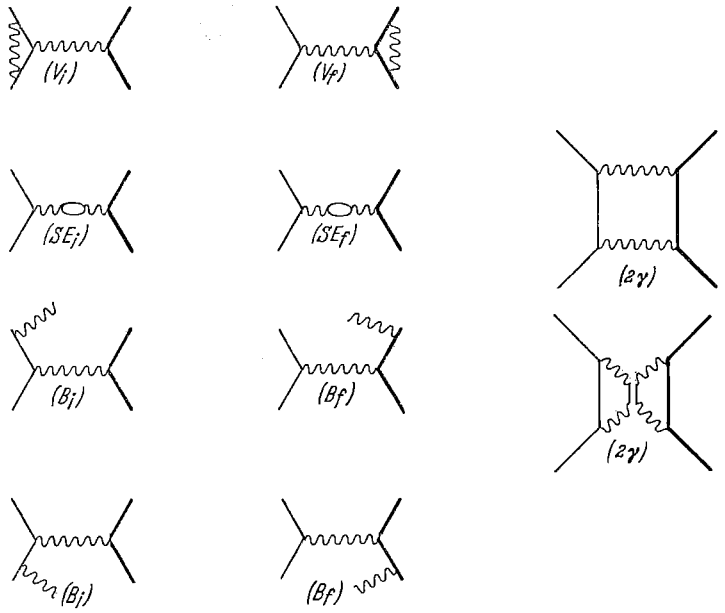

Fig. 11. Lowest order radiative corrections for $e^+ + e^- \to \mu^+ + \mu^-$

most interesting one) there is no interference between the lowest order graph (with only one photon exchanged) and the 2γ graph. Thus to the order e^6 in cross-section one can entirely neglect for such situations the 2γ graphs. Furthermore one can also neglect the interference between initial and final bremsstrahlung .The reason in both cases is the invariance under charge conjugation which does not allow a photon to transform virtually into two photons. One thus sees that one can talk consistently in these cases of an initial (interference of the lowest order graph with $V_i + SE_i$ plus the squared B_i contributions) and a final (same with $i \to f$) radiative correction.

We shall examine here the radiative corrections assuming the following idealized experimental conditions. The muons emitted in $e^+ + e^- \to \mu^+ + \mu^-$ are observed in (approximately) opposite directions at a scattering angle θ. The detection system has an opening angle $\Delta\theta$ and the energy of a muon is observed with an energy resolution $\Delta\varepsilon$. The situation is illustrated in Fig. 12. We first look for the restrictions imposed by the energy resolution $\Delta\varepsilon$ and then for the restrictions imposed by the angular resolution of the detectors. The energy resolution $\Delta\varepsilon$

limits the energy of a bremsstrahlung photon emitted in the direction θ up to a maximum energy $\Delta\varepsilon$. For a photon emitted in the direction orthogonal to the direction θ (i. e. at angles $\theta = \pm\pi/2$) the maximum energy is instead $2\Delta\varepsilon$. In Fig. 12 we have drawed a kind of ellipsoid (with the shorter axis of $\Delta\varepsilon$ and the longer axis of $2\Delta\varepsilon$) which gives for any direction of bremsstrahlung emission the maximum energy that the

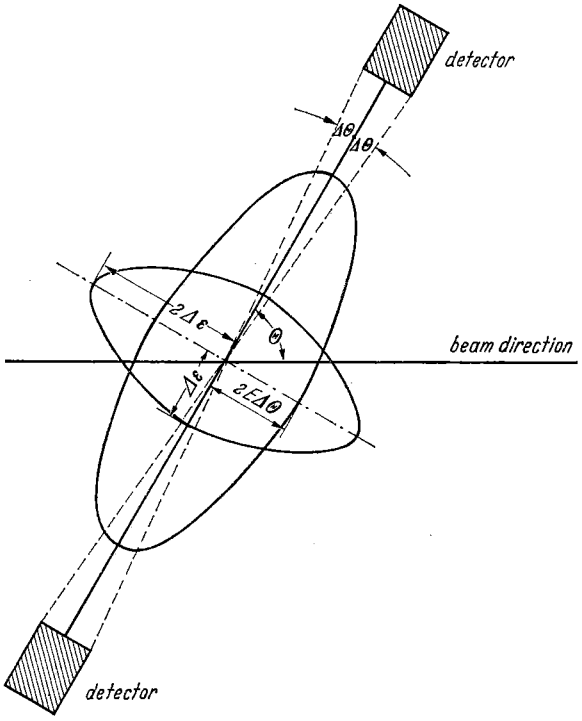

Fig. 12. Energy upper limits for a bremsstrahlung photon for an idealized detection arrangement. In an actual experiment the limits will depend on the particular detectors used

photon can take compatibly with the condition that the final muons have energy between $E - \Delta\varepsilon$ and E. Similarly one can show that the geometrical condition imposed by the detectors implies that the maximum photon energy in the direction θ is $\sim E$ and in the orthogonal direction $\sim 2E\Delta\theta$. The condition gives rise to a limitation, with varying angle, as illustrated in Fig. 12, with the kind of ellipsoid of longer axis E, and shorter axis $\sim 2E\Delta\theta$. We shall assume to be definite $\Delta\varepsilon \sim 2\%$ of E and $\Delta\theta \sim 1°$. The limit $2E\Delta\theta$, is then $\sim 3.5\%$ of E. In Fig. 12 the shadowed region indicates the possible photon momenta (the figure is rotationally invariant around the axis connecting the detectors). Under these conditions the radiative corrections are expected to be large. The physical reason is the following. The correction is almost entirely due to soft photons. The hard photons emitted from the final muons are largely cut-off from the energy resolution. Furthermore, the

muons being relatively heavy particles, their emission is comparably reduced. The hard photons emitted from the electrons are cut-off from the geometrical restrictions for $\theta \sim 90°$, or, for small θ, they are cut-off again by the energy resolution. The integration is to be performed on the shadowed area of Fig. 12, i. e., all photons emitted with energy up to that corresponding to the contour of the shadowed area must be included.

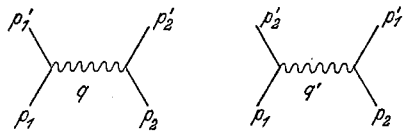

Fig. 13. Graphs for $e^- + e^- \to e^- + e^-$

As usual, one first integrates for an isotropic maximum photon energy, in order to conveniently eliminate the infrared divergencies, and then adds the remaining bremsstrahlung contribution. The "isotropic correction" (which includes also virtual photon corrections) is given by

$$\delta_R(\Delta E) = \frac{\alpha}{\pi}\left\{-\frac{4}{3}\pi^2 - \frac{56}{9} + \frac{26}{3}\ln 2 + \frac{13}{3}\left(\ln\frac{E}{m_e} + \ln\frac{E}{m_\mu}\right) + \right. \\ \left. - 4\left(\ln\frac{E}{m_e} + \ln\frac{E}{m_\mu} + 2\ln 2 - 1\right)\ln\frac{E}{\Delta E}\right\} \tag{23}$$

where ΔE is the isotropic cut-off on the photon energy. The complete integration on the shadowed area has been carried out by G. LONGHI and has given the results:

E (MeV)	δ_R (90°)	δ_R (60°)	δ_R (30°)
200	−19%	−20%	−21%
400	−22%	−23%	−24%
600	−25%	−25%	−26%
800	−26%	−27%	−28%
1200	−28%	−29%	−30%
1500	−30%	−30%	−31%

One expects that, by relaxing the energy resolution, the radiative corrections may decrease in absolute value. The decrease is not however large for θ, say, between 60° and 90° essentially because one is now practically including the hard photons from the muons, which are already down because of the large muon mass.

The problem of higher order corrections is mathematically very complex. An attempt was made to estimate higher order terms by using the method of the renormalization group by FURLAN, GATTO and LONGHI [11].

6. Electron-electron scattering

$$e^- + e^- \to e^- + e^- \tag{24}$$

arises in lowest order from the graphs of Fig. 13. The momentum transfers are both spacelike

$$q^2 = 4E^2 \sin^2 \frac{\theta}{2} \tag{25}$$

$$q'^2 = 4E^2 \cos^2 \frac{\theta}{2} . \tag{26}$$

The Møller formula, modified by the introduction of a form factor F, is, with neglect of the electron mass,

$$\frac{d\sigma}{d(\cos\theta)} = \frac{\pi\alpha^2}{4E^2}\left\{\frac{4 + (1 + \cos\theta)^2}{(1 - \cos\theta)^2}|F(q^2)|^2 + \frac{8}{\sin^2\theta}\mathrm{Re}\,[F^*(q^2)\,F(q'^2)] + \right. \\ \left. + \frac{4 + (1 - \cos\theta)^2}{(1 + \cos\theta)^2}|F(q'^2)|^2\right\} . \tag{27}$$

The form factor F can be thought of as a product $V_e^2\,P_\gamma$, where V_e is the electron-vertex form factor and P_γ is the photon-propagator form factor. For $F = 1$ Eq. (27) takes the simple form

$$\frac{d\sigma}{d(\cos\theta)} = \frac{\pi\alpha^2}{2E^2}\left(\frac{3 + \cos^2\theta}{\sin^2\theta}\right)^2 . \tag{28}$$

Measurements of Møller scattering can be used to probe the theory. If we assume for F

$$F(q^2) = \frac{1}{1 + \frac{q^2}{Q^2}}$$

the relative deviation from the case $F = 1$ is the same as for electron-positron scattering. The maximum deviation again occurs at 90° as for electron-positron scattering. It is important for the interpretation of the experiment to know accurately the radiative corrections. Calculations have been done by TSAI [14] and by BAYER and KHEIFETS [15] under very similar assumptions. These calculations are made by properly taking into account the experimental conditions for the particular colliding beam experiment, and in this respect they differ from other calculations made in view of different (and sometimes irrealizable) conditions. The experiment considered by TSAI (and performed by the Stanford group) is based on the idealized arrangement of Fig. 14. The two detectors for the final electrons are in coincidence. They are centered around the angle θ. Their opening angle is $2\Delta\theta$. They are assumed to have no energy resolution. If a photon is emitted in the direction θ it can take an energy up to the kinematically allowed maximum energy $\sim E$, without being detected. In fact the geometric limits from the detection system do not impose any condition for photons emitted in a direction parallel to the final electrons. However a photon emitted in a direction parallel to the initial particles can only have energy up to ΔE

$$\Delta E = \frac{2E\,\Delta\theta}{\sin\theta + \Delta\theta} \tag{29}$$

consistently with the geometric conditions. The condition (29) is obtained directly from kinematics by considering the configuration for which the

photon energy is maximum compatibly with the condition that the final electron momenta stay inside the two cones subtended by the detectors. For photons emitted along other directions the maximum energy allowed by the apparatus varies with angle. The kind of ellipsoid reported in

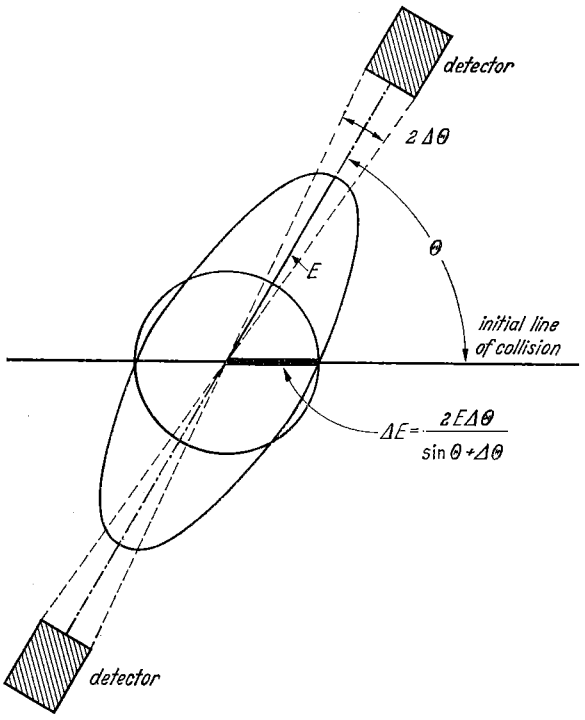

Fig. 14. Energy upper limits for a bremsstrahlung photon in the $e^- - e^-$ scattering experiment

Fig. 14 shows graphically the dependence of the maximum photon energy with photon direction. TSAI's calculations are done by first integrating up to $K_0 = \Delta E$ isotropically. The circle of radius ΔE is reported in Fig. 14. The addition of the "soft" photons with $K_0 < \Delta E$ to the virtual photon radiative corrections removes, as well-known, the dependence on the fictitious photon mass. To these "soft" corrections one then adds the hard photon corrections:

$$d\sigma = d\sigma_{el} + d\sigma_{soft} + d\sigma_{hard} \,. \tag{30}$$

The soft photon correction is well-known. One has

$$\left[\frac{d\sigma}{d(\cos\theta)}\right]_{el} + \left[\frac{d\sigma}{d(\cos\theta)}\right]_{soft} \cong \frac{\pi\alpha^2}{4E^2}\left[\frac{4 + (1+\cos\theta)^2}{(1-\cos\theta)^2} + \frac{4}{\sin^2\theta}\right] \times$$
$$\times \left\{1 - \frac{4\alpha}{\pi}\left[\frac{23}{18} - \frac{11}{12}\ln\left(\frac{2E^2}{m_e^2}(1-\cos\theta)\right)\right] + \right.$$
$$\left. + \left[\ln\left(\frac{E^2}{m_e^2}\sin^2\theta\right) - 1\right]\ln\frac{E}{\Delta E}\right\} + \text{same term with } \cos\theta \to -\cos\theta \,. \tag{31}$$

The integration of the hard portion is much more difficult and has been done by TSAI. For $E = 500$ MeV and $\Delta\theta = 3.5°$ TSAI finds a total correction [defined from $d\sigma = d\sigma_{\text{Møller}}(1 + \delta)$] of -9.5% at 90°, and of -6.0% at 35%. The calculations performed by BAYER and KHEIFETS are claimed to be more accurate. These authors introduce also a threshold resolution E_1 for the detectors: i. e. the detectors do not register electrons

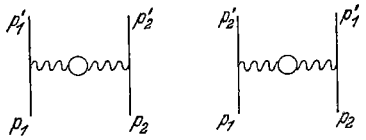

Fig. 15. Vaccum polarization graphs

with energy lower than E_1. Their numerical results are as follows. For $E = 100$ MeV, $E_1 = 50$ MeV and $\Delta\theta = 1.25°$ one has: $\delta\,(40°) = -15.8\%$, $\delta\,(50°) = -17.4\%$, $\delta\,(60°) = -18.3\%$, $\delta\,(70°) = -18.9\%$, $\delta\,(80°) = -19.4\%$, $\delta\,(90°) = -19.6\%$. For $E = 500$ MeV, $E_1 = 10$ MeV, and $\Delta\theta = 3.5°$: $\delta\,(40°) = -10.6\%$, $\delta\,(50°) = -12.1\%$, $\delta\,(60°) = -13.2\%$, $\delta\,(70°) = -13.7\%$, $\delta\,(80°) = -14.1\%$, and $\delta\,(90°) = -14.4\%$. The last choice of the parameters E and $\Delta\theta$ coincides with that of Tsai except for the threshold resolution $E_1 = 10$ MeV. The absolute values for $\delta(\theta)$ obtained by BAYER and KHEIFETS are however larger.

It is interesting to know the relative magnitude of the various contributions from virtual electrons, muons, pion and proton pairs in the vacuum polarization diagrams that contribute to the elastic radiative corrections (Fig. 15). Using known expressions by FEYNMAN [16] and by EUWEMA and WHEELER [17], valid for particles without structure, one sees that in $e^- + e^- \to e^- + e^-$ at $E = 500$ MeV and $\theta = 90°$ (where the contribution is expected to be larger) the vacuum polarization contribution is of 2% for electrons, 0.35% for muons, 0.089% for pions, and 0.02% for protons in the closed loops of Fig. 15.

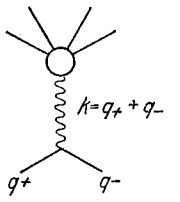

Fig. 16. Annihilation graph

7. The rest of this discussion — except for a few remarks at the end about weak interactions — will concern $e^+ - e^-$ annihilation into strong-interacting-particles. The reactions proceed mostly through one-photon exchange (Fig. 16).

More generally we shall talk of the one-photon channel whenever the interaction passes through one intermediate photon. For experiments that treat the charges symmetrically (such as total cross-sections or, for instance, $e^+ + e^- \to \pi^+ + \pi^-$ at a definite angle but without distinguishing the final charges) the interferences between the one-photon and the two-photon channels vanish on account of charge conjugation invariance. A simple proof is as follows. The interference term between one-photon and two-photon channel has the form

$$\text{Re} \sum_f \langle i\,|S_1|\,f\rangle\,\langle f\,|S_2|\,i\rangle = \text{Re}\,\langle i\,|S_1\,P_f\,S_2|\,i\rangle \tag{32}$$

if S_1 is that part of the S matrix from the one-photon channel and S_2 the part from the two-photon channel. We have called P_f the projector into the final states f. We now assume that the set of states is symmetric under charge conjugation such that

$$C^{-1} P_f C = P_f$$

where C is the charge conjugation operator. Eq. (32) can be written as

$$(32) = \mathrm{Re}\, \langle i_- | S_1 P_f S_2 | i_+ \rangle = \mathrm{Re}\, \langle i_- | C^{-1} S_1 P_f S_2 C | i_+ \rangle = 0$$

where $|i_+\rangle$ and $|i_-\rangle$ are respectively even and odd under charge conjugation and we have noted that $S_1 |i\rangle = S_1 | i_-\rangle$ and $S_2 |i\rangle = S_2 | i_+\rangle$. For processes that go through the one-photon channel the final strong-interacting-particles produced according to

$$e^+ + e^- \to a + b + c + \cdots$$

must be in a state with $P = -1$, $C = -1$, $J = 1$, $T = 1$ or 0. That the final amplitude must transform as a polar vector follows at once by observing that the gauge condition $K_\mu \langle f | j_\mu | 0 \rangle = 0$ on the matrix element of the current j_μ, becomes in c. m., where $K_\mu = (0, K_4)$, $K_4 \langle f | j_4 | 0 \rangle = 0$ implying that the amplitude is given by the polar vector $\langle f | \vec{j} | 0 \rangle$. The one-photon channel selection rules, $P = -1$, $C = -1$, $J = 1$, $T = 1, 0$, are certainly valid to order $e^4 = \alpha^2$ in the intensity, and they are violated from interference with the two-photon channels at order $e^6 = \alpha^3$. However for the symmetrical experiments we have mentioned these interferences vanish and the violation of the selection rules only occurs at order $e^8 = \alpha^4$ in the intensity (one has to add bremsstrahlung corrections). For production of n pions one has to add to the above rules the rule $T = 1$ for n even and $T = 0$ for n odd. A typical feature of two-body annihilation through the one-photon channel is the

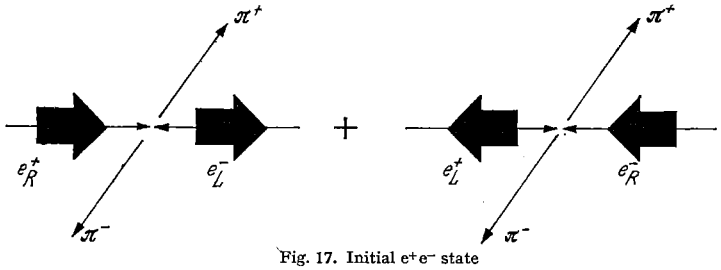

Fig. 17. Initial e^+e^- state

possibility of predicting at any energy the form of the angular distribution in the form $A + B \cos^2\theta$. For annihilation into two spin zero particles (2π, $\eta + \pi$, $2\mathrm{K}$, etc.) the final pions cannot move in the same direction of the incident pair if angular momentum has to be conserved (we are always neglecting the electron mass). In fact in the $m_e = 0$ limit a right-handed electron couples to a left-handed positron and a left-handed electron to a right-handed positron. If the pions were emitted along the collision line the angular momentum projection on the line would be zero in contrast to the initial value of $+1$ or -1 (see Fig. 17). Therefore

$A + B = 1$ and the distribution is proportional to $\sin^2\theta$. Two spinless bosons produced through the one-photon-channel will be in a P-state if their relative parity is positive. Two spin-one bosons of positive relative parity are produced in $1P_1$, $5P_1$ and $5F_1$. A pair of spin $\frac{1}{2}$ particles is produced in $3S_1$ and $3D_2$ for positive relative parity or in $1P_1$ and $3P_1$ if the relative parity is negative. Similarly a pair of a vector meson and a pseudoscalar meson will be produced in relative P state. In the one-photon channel the unitarity limitation on the cross-section takes a special simple form. From the limitation $\sigma_J \leqq \pi \lambda\!\!\!^{-2}(2J + 1)$, which for $J = 1$ gives $\sigma_1 \leqq 3\pi \lambda\!\!\!^{-2}$ we get here the limitation

$$\sigma \leqq \frac{3}{4}\pi \lambda\!\!\!^{-2} \tag{33}$$

for all reactions going through the one-photon channel. The factor $\frac{1}{4}$ comes from the fact that, in the limit $m_e = 0$ only one of the four possible initial $e^+ e^-$ spin states can contribute to the cross-section, namely the state

$$\frac{1}{\sqrt{2}}(|e_L^-, e_R^+\rangle + |e_R^-, e_L^+\rangle) . \tag{34}$$

8. The reaction $e^+ + e^- \to a + b + \cdots$ is especially useful to measure the form factors of the vertex $(\gamma, a + b + \cdots)$ of the strong-interacting-particles a, b, ... for timelike value $K^2 = -4E^2$ of the virtual photon momentum. One important experimental aspect is the unique possibility

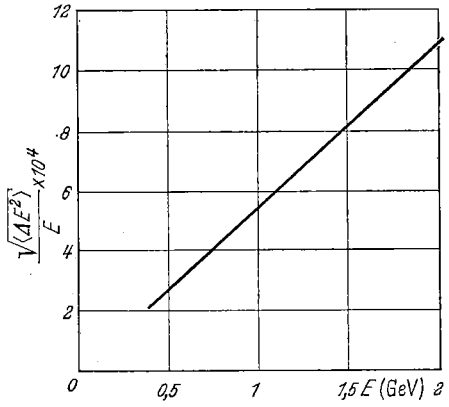

Fig. 18. Predicted energy dispersion of the beam in the Adone project

of disposing of very narrow energy resolutions which will allow measurements of very narrow widths of possible resonances in the cross-sections. The expected energy dispersion of the beam is illustrated in Fig. 18 (I would like to thank F. AMMAN and C. BERNARDINI for kindly providing me with this figure). These resonances are expected to occur when an intermediate boson of $P = -1$, $C = -1$, $J = 1$ and zero strangeness of mass $M^2 = 4E^2$ couples to the initial photon and to the final strong-interacting-particles. Intermediate bosons of different quantum numbers

are expected not to contribute as they do not couple in the dominant one-photon channel. In more detail for a qualitative discussion of the possible resonant contributions we can assume a Breit-Wigner description for the resonance cross-section near its maximum

$$\sigma(E) \cong \pi \lambda\!\!\!^{-2} \frac{2J+1}{4} \frac{\Gamma_i \Gamma_f}{(2E-M)^2 + \frac{\Gamma^2}{4}} \tag{35}$$

where Γ_i and Γ_f are the rates into the initial $e^+ - e^-$ state and the final state respectively. If the energy resolution in c. m. is $2\Delta E$ what one observes is

$$\bar{\sigma}_R = \frac{1}{\Delta E} \int_{\frac{1}{2}(M-\Delta E)}^{\frac{1}{2}(M+\Delta E)} \sigma(E)\, dE\,. \tag{36}$$

If the width is larger than $2\Delta E$, $\Gamma \gg 2\Delta E$, as it will most often occur, at the resonance one will observe

$$\sigma_R = \sigma(2M) = \pi \lambda\!\!\!^{-2}(2J+1)\, B_i\, B_f \tag{37}$$

where B_i and B_f are the branching ratios for decay into the initial and the final state respectively. If there is a dominant final state, $B_f \cong 1$ and the relevant quantity is

$$\frac{\Gamma_i}{\Gamma}\,. \tag{38}$$

The other situation, $\Gamma \ll 2\Delta E$, gives for the observed value

$$\bar{\sigma}_R \cong 2\pi \lambda\!\!\!^{-2} \frac{\pi}{4} (2J+1)\, B_i\, B_f \frac{\Gamma}{2\Delta E}\,. \tag{39}$$

Again, with $B_f \cong 1$, the relevant quantity is

$$\frac{\Gamma_i}{\Delta E}\,. \tag{40}$$

The possibility of observing the resonant contribution thus depends on the value of Γ_i/Γ for a wide (as compared to ΔE) resonance, or on the value of $\Gamma_i/\Delta E$ for a narrow resonance. If $\Gamma \sim \Delta E$ the two parameters coincide and the discussion can be extended also to these cases. Now Γ_i is strongly affected by some factors that can be derived from general considerations. If the resonant state has

$J=0,\ C=\ \ 1$	then	$\Gamma_i \propto \alpha^4 m_e^2$
$J=0,\ C=-1$		$\Gamma_i \propto \alpha^6 m_e^2$
$J=1,\ C=\ \ 1$		$\Gamma_i \propto \alpha^4$
$J=1,\ C=-1$		$\Gamma_i \propto \alpha^2$
$J=2,\ C=\ \ 1$		$\Gamma_i \propto \alpha^4$
$J=2,\ C=-1$		$\Gamma_i \propto \alpha^6$

etc.

These rules can easily be obtained from charge conjugation, angular momentum, and the helicity rule that we have already used before. The biggest effects are for $J = 1$, $C = -1$ (ρ^0, ω^0, φ^0) and next in importance for $J = 1$, $C = 1$ (perhaps A_1^0 (1080) has these quantum numbers; such states however are not visible in 2π annihilation) and $J = 2$, $C = 1$ (perhaps f^0 or A_2^0 (1310)), while for $J = 0$, $C = 1$ (π^0, η^0) there is no hope of an observable effect.

9. Annihilation into n pions through the one-photon channel leads, as we have said, to a final state with $P = -1$, $C = -1$, $J = 1$, $T = 1$ for n even and $T = 0$ for n odd. If $\vec{J}$ is the most general vector (pseudovector) formed out of the independent final momenta for n even (odd) the final distribution can be shown to have the general form

$$\frac{1}{2} |\vec{J}|^2 \sin^2\theta \tag{41}$$

where θ is the angle formed between $\vec{J}$ and the initial line of collision. For annihilation into 2π the only vector is $\vec{p}_1 - \vec{p}_2$ and we get the expected $\sin^2\theta$ distribution. For annihilation into 3π the only pseudovector is the normal to the production plane, and we thus obtain that such a normal has a $\sin^2\theta$ distribution around the initial line of collision. For annihilation (by one-photon exchange) into two spin-less bosons the differential cross-section in c. m. is

$$\frac{d\sigma}{d(\cos\theta)} = \frac{\pi}{16} \alpha^2 \frac{1}{E^2} \beta^3 |F(K^2)|^2 \sin^2\theta \tag{42}$$

where $F(K^2)$ is the e. m. form factor of the boson. The total cross-section is

$$\sigma = \frac{1}{m^2} (0.53 \cdot 10^{-32} \text{ cm}^2) \frac{1}{x^2} \left(1 - \frac{1}{x^2}\right)^{\frac{3}{2}} |F(-4m^2 x^2)|^2 \tag{43}$$

where m is the mass of the boson in GeV and $x = E/m$. Eq. (42) applies to $e^+ + e^- \to \pi^+ + \pi^-$, $e^+ + e^- \to K^+ + K^-$, $e^+ + e^- \to K_1^0 + K_2^0$, etc. The reaction $e^+ + e^- \to \pi^0 + \pi^0$ does not proceed through the one-photon channel. It requires exchange of two photons. The $K^0 \bar{K}^0$ pair produced through one-photon channel must be in a state with $C = -1$. Therefore only $K_1^0 K_2^0$ pairs are produced, but no $K_2 K_2$ or $K_1 K_1$ pairs. From (42) or (43) one can measure the form factor $F(K^2)$ for $K^2 = -4E^2$, starting from the threshold $K^2 = -(2m_\pi)^2$. The form factor is complex in the observed physical region; however its phase cannot be directly determined from the experiment. The annihilation $e^+ + e^- \to \pi^+ + \pi^- + \pi^0$ leads to a final state with $l = L = 1, 3, 5$, etc., where l is the $\pi^+ - \pi^-$ relative angular momentum and L is the π^0 angular momentum relative to $\pi^+ - \pi^-$. One has

$$\frac{d^2\sigma}{d\omega_+ \, d\omega_- \, d(\cos\theta)} = \frac{\alpha}{(2\pi)^2} \frac{1}{64E^2} |H|^2 \sin^2\theta \, (\vec{p}^{(+)} \times \vec{p}^{(-)})^2 \tag{44}$$

where ω_+, ω_- are the energies of π^+, π^- in c. m. and $\vec{p}^{(+)}$, $\vec{p}^{(-)}$ are their momenta; H is a form factor depending on E, ω_+, ω_-, and θ, already defined, is the angle of the normal to the production plane with the

initial line of collision. The dependence of H on its variables will be affected strongly from the existence of the ω meson and of the ρ meson. The ω-meson will be responsible for the expected resonant behaviour for $K^2 = -m_\omega^2$. The possibility of resonant interaction of the final mesons in the $J=1, T=1$ meson resonant state will appreciably affect the final distribution. From such considerations one would suggest to try first with H of the form

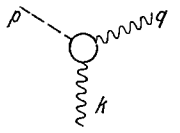

Fig. 19. The $\pi^0 - 2\gamma$ vertex

$$H = \frac{a}{4E^2 - m_\omega^2 + i\, m_\omega\, \Gamma_\omega} \times \sum_i \times \frac{1}{(4E^2 + m_\pi^2 - m_\rho^2 + i\, m_\rho\, \Gamma_\rho)^2 - 4E\,\omega_i} \tag{45}$$

where ω_i is $\omega_+, \omega_-, \omega_0$ for $i = 1, 2, 3$, Γ_ω, Γ_ρ and m_ω, m_ρ are the widths and masses of ω and ρ, and a at a first approximation could be assumed to be roughly constant. The mode $e^+ + e^- \to 3\pi^0$, or in general $\to n\,\pi^0$, is forbidden in the one-photon channel. The annihilation $e^- + e^- \to \pi^0 + \gamma$ through one-photon exchange, would allow the exploration of the $\pi^0 \to 2\gamma$ vertex. This vertex has the form

$$\frac{1}{4} G(-K^2, -q^2, -p^2)\, \varepsilon_{\mu\nu\lambda\varrho} F_{\mu\nu}(q)\, F_{\lambda\varrho}(K) \tag{46}$$

where G is a form factor depending on $K^2 = -4E^2$, the pion momentum p, and the photon momentum q (see Fig. 19). We write $G(-K^2)$ for $G(-K^2, 0, m_\pi^2)$. The π^0 lifetime is given by

$$\frac{1}{\tau} = \frac{m_{\pi^0}^3}{64\pi} |G(0)|^2 \tag{47}$$

and the cross-section for $e^+ + e^- \to \pi^0 + \gamma$ is

$$\frac{d\sigma}{d(\cos\theta)} = \frac{\pi\,\alpha}{m_\pi^3} \frac{1}{\tau} \beta^3 (1 + \cos^2\theta) \left| \frac{G(-K^2)}{G(0)} \right|^2 . \tag{48}$$

Eq. (48) also applies, with the suitable changes, to $e^+ + e^- \to \eta^0 + \gamma$. Annihilation into a fermion-antifermion pair, according to

$$\begin{aligned} e^+ + e^- &\to p + \bar{p}\,, \quad n + \bar{n} \\ &\to \Lambda + \bar{\Lambda} \\ &\to \Sigma + \bar{\Sigma} \\ &\to \Xi + \bar{\Xi} \end{aligned} \tag{49}$$

leads to a final state consisting of $^3S_1$ and $^3D_1$ as long as the process proceeds through the one-photon channel. Near threshold the cross-section will thus be isotropic and will rise $\propto \beta$. The differential cross-section is in general

$$\frac{d\sigma}{d(\cos\sigma)} = \frac{\pi}{8} \alpha^2 \lambda^2 \beta \left[|F_1(K^2)|^2 + \mu\, F_2(K^2)|^2 (1 + \cos^2\theta) + \left| \frac{m}{E} F_1(K^2) + \frac{E}{m} \mu\, F_2(K^2) \right|^2 \sin^2\theta \right] \tag{50}$$

where F_1 and F_2 are the Dirac and Pauli form factors respectively normalized to $F_1(0) = 1$ and $F_2(0) = 1$ for a charged fermion and μ is the static anomalous magnetic moment of the fermion. Along the absorptive cut the form factors are in general complex. The absorptive cut starts at much lower values of K^2 than the physical region for the annihilation. For instance in $e^+ + e^- \to N + \bar{N}$ the absorptive cut starts at $K^2 = -4\,\mu_\pi^2$ for the isovector part and at $K^2 = -9\,\mu_\pi^2$ for the isoscalar part. The fact that the form factors are in general complex in the physical region of the process brings about the existence of a polarization of the final fermions normal to the production plane, already at the lowest electromagnetic order. This situation is opposite to scattering e+ (fermion) $\to$ e + (fermion) where there is no polarization at lowest order. In $e^+ + e^- \to$ (fermion) + (antifermion) the polarization of the fermion is given by $P(\theta)$, where

$$\frac{d\sigma}{d(\cos\theta)} P(\theta) = -\frac{\pi}{8}\alpha^2 \lambda\!\!\!^{-2} \beta^3 \mu \frac{E}{m} \operatorname{Im}[F_2^*(K^2) F_1(K^2)] \sin(2\theta) \qquad (51)$$

and it is directed along $\vec{p} \times \vec{q}_+$ where $\vec{p}$ is the momentum of the final fermion and $\vec{q}_+$ that of the positron. The polarization of the antifermion is $-P(\theta)$. The reactions $e^+ + e^- \to \Lambda^0 + \bar{\Sigma}^0$ and $e^+ + e^- \to \Sigma^0 + \bar{\Lambda}^0$ have a cross-section

$$\frac{d\sigma}{d(\cos\theta)} = \frac{\pi}{8}\alpha^2 \lambda\!\!\!^{-2} \beta \Big\{ \beta^2 \cos^2\theta\, [|f_1(K^2)|^2 + K^2 |f_2(K^2)|^2] + [|f_1(K^2)|^2 - K^2 |f_2(K^2)|^2] \frac{E_\Lambda E_\Sigma + m_\Lambda m_\Sigma}{E^2} - 4 \frac{m_\Lambda E_\Sigma + m_\Sigma E_\Lambda}{E} \times \times \operatorname{Re}[f_1(K^2) f_2^*(K^2)] \Big\} . \qquad (52)$$

The $\gamma\,\Sigma\,\Lambda$ vertex is written as

$$\bar{u}_\Lambda [f_1(K^2)\,\gamma_\nu + f_2(K^2)\,\sigma_{\nu\mu} K_\mu + f_3(K^2)\,K_\nu]\, v_\Sigma \qquad (53)$$

where u_Λ and v_Σ are the spinors and the f's are the form factors. The gauge condition implies in general

$$f_3(K^2) = i \frac{f_1(K^2)}{K^2} (m_\Sigma - m_\Lambda) . \qquad (54)$$

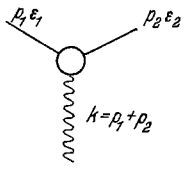

Fig. 20. The electromagnetic vertex of vector mesons

[However f_3 does not enter in (52). This can be seen directly from (53) in c. m. where $\vec{K} = 0$ and by noting that the fourth component of the current vanishes in c. m. from the condition $K_\nu j_\nu = K_4 j_4 = 0$.]

9. Production of a pair of spin one bosons

$$e^+ + e^- \to B + \bar{B}$$

occurs in the states ${}^1P_1$, ${}^5P_1$, and ${}^5F_1$ as can be seen from angular momentum, parity and charge conjugation. The $\gamma B B$ vertex is shown in Fig. 20. The momenta p_1 and p_2 satisfy $p_1^2 = p_2^2 = -m_B^2$ and $(p_1 \varepsilon_1) = (p_2 \varepsilon_2) = 0$.

The general form of the current is

$$J_\mu = \frac{e}{(4\omega_1\omega_2)^{1/2}}\Big\{G_1(\varepsilon_1\varepsilon_2)\,p_\mu + [G_1 + \mu G_2 + \varepsilon G_3]\times \\ \times[(\varepsilon_1 K)\,\varepsilon_{2\mu} - (\varepsilon_2 K)\,\varepsilon_{1\mu}] + \\ + \varepsilon\,\frac{1}{m_B^2}G_3[(K\varepsilon_1)\,(K\varepsilon_2) - \frac{1}{2}K^2(\varepsilon_1\varepsilon_2)]\,p_\mu\Big\} \tag{55}$$

where ω_1 and ω_2 are the c. m. energies of B, $\overline{\mathrm{B}}$; $e\,G_1$, $\mu\,G_2$, $\varepsilon\,G_3$ describe the charge, the magnetic moment and the electric quadrupole moment distributions of B ($\mu+\varepsilon$ and 2ε are the static magnetic moment and electric quadrupole moment respectively). The G's are functions of K^2. The cross-section is

$$\frac{d\sigma}{d(\cos\theta)} = \frac{\pi}{16}\alpha^2\lambda^2\beta^3\Big\{2\left(\frac{E}{m_B}\right)^2|G_1+\mu G_2+\varepsilon G_3|^2(1+\cos^2\theta)+ \\ +\sin^2\theta\left[2\left|G_1+2\left(\frac{E}{m_B}\right)^2\varepsilon G_3\right|^2+\left|G_1+2\left(\frac{E}{m_B}\right)^2\mu G_2\right|^2\right]\Big\}. \tag{56}$$

The β^3 dependence (β is the final velocity) is typical of P-state production. With $G_1=1$, $G_2=G_3=0$ the total cross-section is

$$\sigma = m_B^{-2}(2.1\cdot 10^{-32}\ \mathrm{cm}^2)\,\frac{3}{4}(1-u)^{\frac{3}{2}}\left(\frac{4}{3}+u\right) \tag{57}$$

where m_B is in MeV and u is $(m/E)^2$. The cross-section (57) violates unitarity at high energies. In fact it goes to a constant value when $E\to\infty$ (i. e. $u\to 0$). On the other hand our unitarity limitation, Eq. (33), for the one-photon channel decreases with energy proportionally to $\lambda^2 = E^{-2}$. Although in general one would expect that the form factors in (56) [which have been ignored in (57)] will produce the required damping much before the unitarity limit is reached or the one-photon-channel approximation is unapplicable, the production of weak-interacting-vector mesons might with a good approximation be represented by the cross-section (57). In fact such bosons are not supposed to have strong interactions and their interaction with photons could well be approximated with that of point charges up to rather high energies. The violation of unitarity, by comparing Eq. (33) with Eq. (57) would in any case occur only at $E\sim 100\,m_B$. The total cross-section, from Eq. (57), is given in Fig. 21 for various values of m_B as a function of $x = E/m_B$. One sees that if one could dispose of colliding $e^+ - e^-$ beams of sufficiently high energy it would not be difficult to improve the present lower limit on the mass of the intermediate vector mesons.

10. Experimental investigations about the limits of validity of quantum electrodynamics may eventually run into the difficulty of having to deal with effects of the same order as the effects originating from virtual strong interacting particles. These effects are hard to estimate accurately. It may be relevant to note that direct measurements of the production of strong interacting particles in $e^+ - e^-$ collisions can directly be related to quantities that express the effect of virtual strong

interacting particles on the electrodynamic parameters. The modification to the photon propagator can be expressed through a function $\pi(K^2)$,

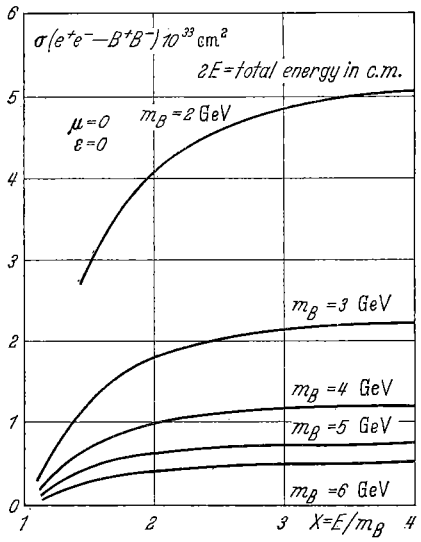

Fig. 21. Total cross-section for annihilation into a vector meson pair

additive with respect to the contributions from the various virtual states [18]. The modified photon propagator can be written as

$$D'_{\mu\nu}(K) = \delta_{\mu\nu}\frac{1}{K^2} + \left(\delta_{\mu\nu} - \frac{K_\mu K_\nu}{K^2}\right)\int_0^\infty \frac{\mathrm{d}a\,\pi(-a)}{a(K^2 + a - i\varepsilon)} \tag{58}$$

where

$$\pi(K^2) = -\frac{(2\pi)^3}{3K^2}\sum_{\substack{Z \\ p_Z = K}} \langle 0|j_\nu(0)|Z\rangle\langle Z|j_\nu(0)|0\rangle . \tag{59}$$

In (59) j_ν is the current operator and the sum is extended over all physical states with momentum $p^{(Z)} = K$. We consider the annihilation of $e^+ + e^-$ into a set of states Z and call $\sigma_Z(E)$ the total cross-section for such annihilations. Similarly we call $\pi_Z(-4E^2)$ the contribution to (59) from the set of states Z. One can formally show that

$$\pi_Z(-4E^2) = \frac{E^2}{\pi^2\alpha}\sigma_Z(E) . \tag{60}$$

Eq. (60) is obtained by direct comparison of the two expressions (59) and the usual expression for $\sigma_Z(E)$. The amplitude for $e^+ - e^-$ annihilation into a final state f, including lowest order vacuum polarization effects due to strong interacting particles, can be written as

$$A(e^+ e^- \to f) = \left[1 + K^2\int_0^\infty \frac{\mathrm{d}a\,\pi(-a)}{a(K^2 + a - i\varepsilon)}\right]\frac{2\pi e}{K^2}(\bar{v}\gamma_\nu u)\langle f|j_\nu(0)|0\rangle \times$$
$$\times\,\delta(p^{(+)} + p^{(-)} - p^{(f)}) . \tag{61}$$

The cross-section for $e^+ + e^- \to f$ is thus modified, by inclusion of vacuum polarization effects due to strong interacting particles at lowest electromagnetic order, by the multiplicative factor

$$\mathfrak{F}(E) = \left| 1 - 4E^2 \int_0^\infty \frac{da\, \pi(-a)}{a(-4E^2 + a - i\varepsilon)} \right|^2 . \tag{62}$$

We are particularly interested in the contribution to (62) from strong resonant states with the appropriate quantum numbers to couple to $e^+ - e^-$ at lowest e. m. order. We call the mass of the resonance M, its full width Γ, and B its branching ratio for decay into $e^+ - e^-$. For a rough estimate of $\mathfrak{F}(E)$ we approximate the resonant cross-section in the neighbourhood of the resonance with a Breit-Wigner formula

$$\sigma_R(E) = \pi \lambda\!\!\!^{-2} \frac{3}{4} B \frac{\Gamma^2}{(2E - M)^2 + \frac{1}{4}\Gamma^2} . \tag{63}$$

From (62), (60), and (63) one can derive an approximate expression for the resonant contribution to $\mathfrak{F}(E)$

$$\mathfrak{F}_R(E) \cong \left| 1 - \frac{3}{2} \alpha\, b \frac{\Gamma}{M - 2E - i\frac{\Gamma}{2}} \right|^2 \tag{64}$$

where we have introduced $b = B/\alpha^2$ to exhibit clearly the electromagnetic order. For a narrow resonance such that $\Gamma \ll \Delta E$ the effect will have to be averaged over ΔE giving

$$\overline{d\sigma} = \left[1 + \frac{\Gamma}{\Delta E} (1 + 9\alpha^2 b^2) \frac{\pi}{4} \right] d\sigma_0 \tag{65}$$

where $d\sigma_0$ is the lowest order cross-section. For a sufficiently wide resonance one can hope to measure $\mathfrak{F}(E)$ as given by (64). It can be seen that $\mathfrak{F}(E)$ has a maximum at about $2E = M + \frac{1}{2}\Gamma$ and a minimum at about $2E = M - \frac{1}{2}\Gamma$ where it reaches the values

$$1 + 3\alpha b \quad \text{and} \quad 1 - 3\alpha b \tag{66}$$

respectively. For the ω-meson, assuming a branching ratio of $1.0 \cdot 10^{-4}$ [19] for the decay mode $\omega \to e^+ + e^-$ we find that $\mathfrak{F}_{max} - 1$ from the ω resonance is $\sim 0.5 \cdot 10^{-1}$, which is much larger than other non-resonant contributions to vacuum polarization, but still of the order of the radiative corrections for the usual experimental arrangements. For the ρ meson with $B \sim 0.5 \cdot 10^{-4}$ one finds again an effect of $4 \cdot 10^{-2}$. However for the ρ meson, with a branching ratio into lepton pairs of $\sim 1.0 \cdot 10^{-3}$ the effect is expected to be very large, of the order of 30%.

11. We shall now look more closely at the annihilation modes into 2π, 3π, 2K, and $\pi^0 + \gamma$, going through the known meson resonances. I shall report on some computations done with G. ALTARELLI and E. CELEGHINI.

Let us first discuss the particularly simple case of $e^+ + e^- \to (\rho^0) \to$ $\to \pi^+ + \pi^-$. We shall describe this process by the graph of Fig. 22.

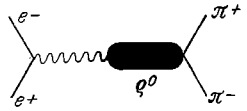

Fig. 22. The ρ^0 resonant contribution to $e^- + e^+ \to \pi^+ + \pi^-$

For its evaluation we need the $\gamma_{\rho\gamma}$ coupling constant of ρ^0 to a photon and the γ_ρ coupling constant of ρ^0 to $\pi^+ + \pi^-$. The two couplings are related as was shown by GELL-MANN and ZACHARIASEN [20] and by R. DASHEN and D. SHARP [21] by

$$\gamma_{\rho\gamma} = \frac{e\, m_\rho^2}{2\gamma_\rho} .$$

In general a similar situation is met when a meson (in this case ρ) is coupled to a current (in this case the isotopic spin current), which is in its turn coupled to the photon with the universal strength e. With such a model in the $e^+ + e^- \to (\rho^0) \to \pi^+ + \pi^-$ amplitude the coupling-constants $\gamma_{\rho\gamma}$ and γ_ρ cancel out and one has

$$\sigma = \frac{\pi\,\alpha^2}{12}\,\beta^3\,\frac{1}{E^2}\,\frac{m_\rho^4}{[(4E^2 - m_\rho^2)^2 + m_\rho^2\,\Gamma_\rho^2]} . \tag{67}$$

If calculated at resonance σ becomes

$$\sigma_R = \frac{\pi\,\alpha^2}{3}\,\beta^3\,\frac{1}{\Gamma_\rho^2} . \tag{68}$$

This formula may be compared with what one gets from a Breit-Wigner formula at the resonance

$$\sigma_{R\,(\text{Breit-Wigner})} = \frac{12\pi}{m_\rho^2}\,\frac{\Gamma_{e^+e^-}}{\Gamma_\rho} .$$

The proportionality in Eq. (68) to Γ_ρ^{-2} reflects the fact that $\Gamma_{e^+e^-}$ is inversely proportional to Γ_ρ : $\Gamma_{e^+e^-} \propto \alpha^2 m_\rho \left(\frac{m_\rho}{\Gamma_\rho}\right)$ such that $\sigma_{R(\text{Breit-Wigner})}$ $\propto \frac{1}{m_\rho^2}\,\alpha^2 m_\rho \left(\frac{m_\rho}{\Gamma_\rho}\right)\frac{1}{\Gamma_\rho} \sim \frac{\alpha^2}{\Gamma_\rho^2}$. Such an inverse proportionality of $\Gamma_{e^+e^-}$ to Γ_ρ follows from the expression of $\gamma_{\rho\gamma}$. Note also that Eq. (67) can be derived also from a direct dispersion theoretic approach if one neglects 4π intermediate states and takes a Breit-Wigner shape for the resonating two-pion p-wave. Numerically with $\Gamma_\rho = 106$ MeV one gets from Eq. (68)

$$\sigma_R = 1.6 \cdot 10^{-30}\ \text{cm}^2 \quad (\text{with } \Gamma_\rho = 106\ \text{MeV}) .$$

Independently one can use directly the Breit-Wigner prediction and insert for $\Gamma_{e^+e^-}$, the width for $\rho \to e^+ e^-$ in the empirical number given by ZDANIS et al. [19]. With the quoted experimental errors one finds

$$\sigma_R \sim \text{between } (0.4 \text{ and } 2.5) \times 10^{-30}\ \text{cm}^2$$

not in contradiction with the above (completely theoretical) prediction. The same kind of argument can be applied to the reaction $e^+ + e^- \to$ $\to (\varphi^0) \to K^+ + K^+$ described by Fig. 23. At the $\varphi - \gamma$ vertex we insert $\gamma_{\varphi\gamma}$ and at the $\varphi \to K^+ K^-$ vertex we insert the coupling constant f_φ.

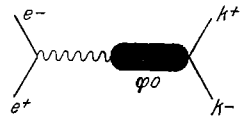

Fig. 23. The φ^0 resonant contribution to $e^+ + e^- \to K^+ + K^-$

The calculation of $\gamma_{\varphi\gamma}$ goes along the following line. One thinks of the physical φ as a superposition of the octet member φ_0 and the unitary singlet ω_0

$$\varphi = \cos\theta\ \varphi_0 + \sin\theta\ \omega_0 .$$

The e. m. current in SU_3 is supposed to have octet behaviour (except for special kinds of triplet models). This means that it cannot couple invariantly to φ_0; it is only coupled to φ_0. Now φ_0 is supposed to be coupled to the hypercharge current, with a strength that we call f_Y. Thus the coupling of φ_0 to the photon follows from the argument reported before for the case of ρ. If we then call $\cos\theta = a$ (and later on $\sin\theta = b$) we have

$$\gamma_{Y\varphi} = -a \frac{e\, m_\varphi^2}{2 f_Y}$$

(we have put m_φ^2 in the numerator for $m_{\varphi_0}^2$, without any appreciable error). The value f_Y can be obtained from f_ρ as φ_0 and ρ are members of the same vector meson octet. With such a model

$$\sigma = \frac{\pi\,\alpha^2}{12}\, a^2 \left(\frac{f_Y^2}{4\pi}\right)^{-1} \left(\frac{f_\varphi^2}{4\pi}\right) \frac{\beta^3}{E^2} \frac{m_\varphi^4}{[(4E^2 - m_\varphi^2)^2 - m_\varphi^2\, \Gamma_\varphi^2]} . \qquad (69)$$

For Γ_φ we assume $\Gamma_\varphi \cong 3.1$ MeV and we can obtain, from its value, f_φ^2 on the assumption that φ^0 decays mostly into 2K. At resonance we thus find, from (69),

$$\sigma_R = 0.5 \cdot 10^{-29}\ \mathrm{cm}^2 .$$

Similarly for $e^+ + e^- \to K^0 + \bar{K}^0$ we find $\sigma_R = 0.34 \cdot 10^{-29}\ \mathrm{cm}^2$. For $e^+ + e^- \to (\omega^0) \to \pi^+ \pi^- \pi^0$ the model is represented by Fig. 24.

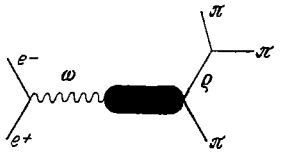

Fig. 24. The ω^0 resonant contribution to $e^+ + e^- \to 3\pi$

We need $\gamma_{\omega\gamma}$ that we can take, by the same argument used with φ, from the expansion $\omega = -\sin\theta\ \varphi_0 + \cos\theta\ \omega_0$ and from the $\varphi_0 - \gamma$

coupling

$$\gamma_{\omega\gamma} = b\frac{e\,m_\omega^2}{2f_\gamma}\,.$$

We also need $f_{\omega\rho\pi}$ that is calculated (see for instance the paper by DASHEN and SHARP) from the ω-width (taken ~ 9.5 MeV) assuming that $\omega \to 3\pi$ goes as $\omega \to \rho + \pi \to (2\pi) + \pi$. Let us consider the particular configuration with the 3π emitted in $e^+ + e^- \to 3\pi$ of equal energies in c. m. at 120° degrees with respect to each other and lying in a plane containing the colliding beam direction. The choice of this particular configuration is suggested by the consideration of the $\sin^2\theta$ dependence of the normal to the final 3π plane with respect to the incident momenta, which gives maximum probability for a final plane containing the initial momenta. Furthermore the maximum probability with respect to the final variables in the plane is obtained for an equilateral triangle configuration, of the final pion momenta. For such a configuration at the resonance

$$\frac{d\sigma}{d\omega_+\, d\omega_-} = 0.7 \cdot 10^{-28}\ \text{cm}^2/(\text{GeV})^2\,.$$

For the total cross-section at resonance we find $\sigma_R = 1.7 \cdot 10^{-30}$ cm^2. We also note that with a Breit-Wigner expression and with the empirical $\omega \to e^+ + e^-$ rate we obtain a total cross-section for $e^+ + e^- \to 3\pi$, at the resonance, of $(0.4-4.7) \cdot 10^{-30}$ cm^2, where the uncertainty is that suggested by the given experimental error of the $\omega \to 2e$ rate of ZDANIS et al. It is an interesting topic to study the effect of addition of two photon exchange terms. Let us consider $e^+ + e^- \to \pi^+ + \pi^-$ and assume that one photon exchange goes entirely through the intermediate ρ^0, in the way we have already discussed. When considering two-photon exchange, at order α^4, we expect pole contributions from $J = 1$, $C = 1$ mesons and $J = 2$, $C = 1$ mesons. However a $J = 1$, $C = 1$ meson cannot decay into 2π (two pions in $l = 1$ have $C = -1$). Possible $J = 2$, $C = 1$ mesons are f^0 and $A_2(1310)$. We shall discuss here the f^0 contribution.

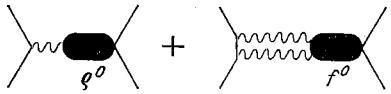

Fig. 25. Addition of two photons contribution to $e^+ + e^- \to 2\pi$

The model is shown in Fig. 25. We assume tentatively a direct $f^0 \to 2e$ coupling of the kind

$$\frac{i\,g}{8}\{[\partial_\nu\bar{\psi},\gamma_\mu\psi] - [\bar{\psi}\gamma_\mu,\partial_\nu\psi] + (\mu\to\nu)]\,C^{\mu\nu}$$

where $C^{\mu\nu}$ describes f^0 and ψ the electron field. For g we make a guess: $g \sim e^4/\pi^2\, m_{f^0}$. The $f^0 \to 2\pi$ width is taken ~ 90 MeV. The general form of the differential cross-section will be (independently of course of the preceding special assumptions)

$$\frac{d\sigma}{d(\cos\theta)} \sim (A + B\cos\theta + C\cos^2\theta)\,\sin^2\theta\,.$$

We see that the $\sin^2\theta$ factor persists also with two photon exchange, in accordance with our helicity arguments (which are independent of the assumption of single γ exchange). The total cross-section for $e^+ + e^- \to \to \pi^+ + \pi^-$ is now

$$\sigma = \frac{4}{3} A + \frac{4}{15} C$$

(no interference between 1γ channel and 2γ-channel for symmetric experiments) and C is also related to $\sigma_{2\pi^0}$ (which only goes through 2γ)

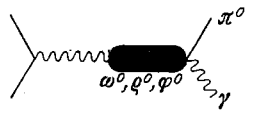

Fig. 26. Resonant contributions to $e^+ + e^- \to \pi^0 + \gamma$

by $\sigma_0 = \frac{2}{15} C$. On the special assumption for the $f^0 \to e^+ + e^-$ coupling reported above we find at the f^0 pole $A \cong 3 \cdot 10^{-33}$ cm^2, $B \cong 1 \cdot 10^{-33}$ cm^2, $C \cong 1 \cdot 10^{-33}$ cm^2. The 2γ effect seems thus to be possibly of the same order as the 1γ effects (provided the assumption made of coupling only through a ρ^0 is verified). In any case the 2γ effect could perhaps be observable when the techniques will have reached a good stage of precision. Let us discuss next the $e^+ + e^- \to \pi^0 + \gamma$ reaction near the contributing poles ω^0, ρ^0, and φ^0. The diagrams are of the kind of Fig. 26. The couplings $\gamma_{\rho\gamma}$, $\gamma_{\omega\gamma}$, and $\gamma_{\varphi\gamma}$ are the same as before. We take the couplings $f_{\omega\pi\gamma}$, $f_{\rho\pi\gamma}$, and $f_{\varphi\pi\gamma}$ from the work of DASHEN and SHARP. The constant $f_{\omega\pi\gamma}$ is calculated assuming that the $\gamma \to \omega\,\pi$ transition goes through a ρ giving $f_{\omega\pi\gamma} \approx \gamma_{\rho\gamma} f_{\omega\rho\pi}/m_\rho^2 = e\, f_{\omega\rho\pi}/f_\rho (f_\rho = 2\gamma_\rho)$. Similarly $f_{\rho\pi\gamma}$ is assumed to go through a Y and one obtains $f_{\rho\pi\gamma} = \gamma_{\mathrm{Y}\gamma} \frac{1}{m_\mathrm{Y}^2} f_{\rho\mathrm{Y}\pi} = e(a\, f_{\varphi\rho\pi} - b\, f_{\omega\rho\pi})/2 f_\mathrm{Y}$. Finally, by the same procedure, $f_{\varphi\pi\gamma} = e\, f_{\varphi\rho\pi}/f_\rho$. The coupling $f_{\omega\rho\pi}$ is obtained from the $\omega \to 3\pi$ width. The coupling $f_{\varphi\rho\pi}$ is not well known [from the $(\varphi \to \rho\,\pi)/(\varphi \to \mathrm{K}\,\overline{\mathrm{K}})$ branching ratio one obtains $f^2_{\omega\rho\pi}/f^2_{\varphi\rho\pi} \sim 850$)]. The model gives the following results. Around the ω resonance

$$\sigma = \frac{1}{24}\pi\,\alpha^2\, b^2 \frac{f^2_{\omega\pi\gamma}}{f^2_\mathrm{Y}} \frac{|\vec{p}|^3}{E^3} \frac{m^4_\omega}{(4E^2 - m^2_\omega)^2 + m^2_\omega\, \Gamma^2_\omega}\,.$$

With $f_{\omega\pi\gamma} = e\, f_{\omega\rho\pi}/f_\rho = (9.2 \pm 0.9) \cdot 10^{-1}\,\mathrm{GeV}^{-1}$ and $\Gamma_\omega = 9.5$ MeV one obtains at resonance $\sigma_\mathrm{R} = 3 \cdot 10^{-31}$ cm^2. For $\pi^0 + \gamma$ from the ρ^0 resonance one has similarly

$$\sigma = \frac{1}{6}\pi\,\alpha^2 \frac{f^2_{\rho\pi\gamma}}{f^2_\rho} \frac{|\vec{p}|^3}{E^3} \frac{m^4_\rho}{(4E^2 - m^2_\rho)^2 + m^2_\rho\, \Gamma^2_\rho}\,.$$

With $f_{\rho\pi\gamma} = e\, f_{\mathrm{Y}\rho\pi}/(2 f_\mathrm{Y}) = 5.6 \cdot 10^{-1}\,\mathrm{GeV}^{-1}$ at resonance one has $\sigma = 7.5 \cdot 10^{-33}$ cm^2. Finally around the φ^0 resonance

$$\sigma = \frac{1}{24}\pi\,\alpha^2\, a^2 \frac{f^2_{\varphi\pi\gamma}}{f^2_\mathrm{Y}} \frac{|\vec{p}|^3}{E^3} \frac{m^4_\varphi}{[(4E^2 - m^2_\varphi)^2 + m^2_\varphi\, \Gamma^2_\varphi]}$$

and with $f_{\varphi\pi\gamma} = e\, f_{\varphi\rho\pi}/f_\rho = (3.1 \pm 0.3) \cdot 10^{-2}\,\mathrm{GeV}^{-1}$ one finds $\sigma = 0.85 \cdot 10^{-31}\,\mathrm{cm}^2$.

12. I shall add some further remarks about weak interactions. We have already discussed the possible pair production of the intermediate bosons with colliding beams of sufficiently high energy. A check of the existence of a possible neutral semiweakly-interacting vector boson can be carried out with $e^+ - e^-$ beams of lower energy. If such a meson, B^0, exists and is coupled to neutral lepton currents it can show off as a resonance in

$$e^+ + e^- \to B^0 \to e^+ + e^-$$
$$e^+ + e^- \to B^0 \to \mu^+ + \mu^- .$$

Such resonances could lead to observable effects in spite of the fact that two semi-weak couplings are involved. The resonance being very narrow one will measure the average cross-section

$$\bar{\sigma}_R = \frac{3}{2}\pi^2 \lambda\!\!\!^{-2} B_i B_f \frac{\Gamma}{2\Delta E} .$$

Let us compare this cross-section to the (purely electrodynamic) cross-section $\sigma_0(2\mu)$ of $e^+ + e^- \to \mu^+ + \mu^-$ at high energy, which, for $E \gg m_\mu$, is $\sim \frac{1}{3}\pi\,\alpha^2\,\lambda\!\!\!^{-2}$. We find

$$\frac{\bar{\sigma}_R(B^0)}{\sigma_0(2\mu)} = \frac{9}{2}\pi\, B_i B_f \left(\frac{\Gamma}{2\Delta E}\right)\frac{1}{\alpha^2}$$

where B_i and B_f are the branching ratios of B^0 into the initial and final state. Consider $e^+ + e^- \to \mu^+ + \mu^-$ and take $B_i \cong B_f \cong \frac{1}{5}$. A typical semiweak Γ corresponds to a few hundreds of eV. Take $\Gamma \sim 0.5 \cdot 10^{-3}$ MeV and $2\Delta E \sim 5$ MeV. One finds

$$\frac{\bar{\sigma}_R(B^0)}{\sigma_0(2\mu)} \cong 1$$

showing that the resulting effect would indeed be very large. From local weak interactions of typical weak strength we do not expect strong effects unless the colliding beams have an energy larger than ~ 10 BeV. For instance a weak lepton interaction of the form $(\mu^+\mu^-)(e^+e^-)$, if it exists, would give a coherent addition to the electromagnetic amplitude for $e^+ + e^- \to \mu^+ + \mu^-$. This small contribution will increase fastly with energy and bring about a $\cos\theta$ term in the angular distribution:

$$\frac{d\sigma}{d(\cos\theta)} \cong \frac{\pi}{8}\alpha^2\,\lambda\!\!\!^{-2}[(1+\cos^2\theta)(1+\varepsilon) + 2\varepsilon\cos\theta]$$

where $\varepsilon \cong 6.2 \cdot 10^{-4}(E/M_N)^2$ (M_N = nucleon mass), if one assumes a weak coupling of the same strength of the β-coupling constant G. The $\cos\theta$ term would however also arise from interference of one-photon and two-photon exchange graphs. A typical parity-non-conserving effect like the longitudinal muon polarization would however be a clear-cut test

for a weak interaction. The final $\mu^{\pm}$ longitudinal polarization is

$$P^{\pm} \cong \pm \varepsilon \frac{(1 + \cos\theta)^2}{1 + \cos^2\theta} .$$

Only for energies $E \sim 30$ GeV, E becomes of order unity and the polarization effect would be large.

In conclusion I would like to thank Doctors G. ALTARELLI, E. CELEGHINI and G. LONGHI for their precious collaboration to the preparation of these notes and to some of the calculations reported.

References

[1] DRELL, S. D.: Ann. phys. **4**, 75 (1958)
[2] — and J. W. MCCLURE: To be published
[3] BAYER, V. N., and V. M. GALITSKY: Physics Letters **13**, 355 (1964)
[4] YENNIE, D. R., S. C. FRAUTSCHI, and H. SUURA: Ann. phys. **13**, 379 (1961)
[5] TSAI, Y. S.: Phys. Rev. **137**, 730 (1965)
[6] ANDREASSI, G., G. CALUCCI, G. FURLAN, G. PERESSUTTI, and P. CAZZOLA: Phys. Rev. **128**, 1425 (1962); see also ANDREASSI, G., P. BUDINI, and G. FURLAN: Phys. Rev. Letters **8**, 184 (1962)
[7] ERIKSSON, K. E., and A. PETERMANN: Phys. Rev. Letters **5**, 446 (1960) ERIKSSON, K. E.: Nuovo cimento **19**, 1044 (1961)
[8] BERNARDINI, C., G. F. CORAZZA, G. DI GIUGNO, J. HAISSINSKI, P. MARIN, R. QUERZOLI, and B. TOUSCHEK: LNF — 64/33
[9] GARYBIAN, G. M.: Izvest. Akad. Nauk. Armenyan. S.S.R. **5**, 3 (1952)
[10] ALTARELLI, G., and F. BUCCELLA: Nuovo cimento **34**, 1337 (1964)
[11] FURLAN, G., R. GATTO, and G. LONGHI: Physics Letters **12**, 262 (1964)
[12] MOSCO, U.: Nuovo cimento **33**, 115 (1964)
[13] LONGHI, G.: Nuovo cimento **35**, 1122 (1965)
[14] TSAI, Y. S.: Phys. Rev. **120**, 269 (1960)
[15] BAYER, V. N., and S. A. KHEIFETS: Nuclear Phys. **47**, 313 (1963)
[16] FEYNMAN, R. P.: Phys. Rev. **76**, 769 (1949)
[17] EUWEMA, R., and J. A. WHEELER: Phys. Rev. **103**, 803 (1965)
[18] KÄLLEN, G.: Quantenelektrodynamik, in Handbuch der Physik, Band V, Teil 1. Berlin-Göttingen-Heidelberg: Springer 1958
[19] ZDANIS, R. A., L. MADANSKY, R. W. KRAEMER, S. HERTZBACH, and R. STRAND: Phys. Rev. Letters **14**, 721 (1965)
[20] GELL-MANN, M., and F. ZACHARIASEN: Phys. Rev. **124**, 965 (1961)
[21] DASHEN, R., and D. SHARP: Phys. Rev. **133**, 1585 (1964)

Prof. Dr. R. GATTO
Istituto di Fisica dell'Università, Firenze and
Laboratori Nazionali del C.N.E.N. di Frascati, Roma